JOURNAL OF MATERIALS SCIENCE 40 (2005) 693–700

# Monte Carlo study of quantitative analysis method of trace elements in thin aluminum films

Y. OSADA
*Nikkei Analytical Center Ltd., 1-34-1 Kambara, Ihara-gun, Shizuoka-ken 421-3291, Japan*
*E-mail: yoshio-osada@nikkeikin.co.jp; chouta@thn.ne.jp*

We have suggested a quantitative analysis method for the determination of trace elements (100–1200 mass ppm) in thin Al films. One of the features of this method is to use calibration curves (K-ratio vs mass ppm in bulk targets) obtained using a Monte Carlo (MC) simulation of electron scattering. First, we verified the calibration curves using bulk standard Al-Cu alloys. As a result, good agreement was obtained with chemical analysis results. Consequently, we confirmed that the MC simulation correctly expressed the electron trajectories in the targets. Here the X-ray generation ratio was defined as the ratio between the X-ray production from an element in a film and the X-ray production by the same element in the same bulk sample. After that, using this MC simulation, we investigated the relation among the X-ray generation ratio, the trace element concentration and the Al film thickness. As a result, we found that the X-ray generation ratio is in relation to the film thickness, however it is not in relation to the concentration of trace element. Namely, if the thickness of unknown samples is known, using the X-ray generation ratio we can transfer from relative X-ray intensity of the film into the relative X-ray intensity of the bulk sample. Also, from the relation that the K-ratio is corresponding to the relative X-ray intensity, using the calibration curves (K-ratio vs mass ratio in bulk targets), we can obtain the concentration (mass ppm) in thin films. Further, in this study, we provided the X-ray generation ratios and the calibration curves of trace elements such as Mg, Si, Ti, Cr, Mn, Fe, Ni, Cu, Zn in the bulk Al matrix.

## 1. Introduction

So far, to analyze the trace elements in thin films, the transmission electron microscope with EDX (TEM/EDX), the secondary ion mass spectrometer (SIMS) and the X-ray photoelectron spectrometer (XPS) have been mainly used. Also, for bulk samples the electron probe microanalyzer (EPMA) and the scanning electron microscope with the energy dispersive X-ray detector have been mainly used. Among those the EPMA with a wavelength dispersive spectrometer is one of the most useful instruments for measuring the analytical composition (mass ppm). In EPMA, there are two quantitative analysis methods for measuring the trace elements of bulk samples. The one is a ZAF method. The ZAF method is the most widely used method of quantitative analysis for bulk samples, where Z, A and F refer to atomic number, absorption, and secondary fluorescence effects, respectively. The other is a calibration curve method. However if the films are thinner than a generated X-ray region, the ZAF method cannot be used, namely it is inapplicable to thin films. The calibration curve method is very laborious since the standard samples must be prepared which resemble the chemical compositions of unknown samples, further it becomes more difficult to make the thin standard films. In the near future it will be desired to analyze the trace elements in thin Al films. To solve this problem, an application of Monte Carlo (MC) simulation to the determination of the calibration curves is one of the most effective approaches. In this study we verified the calibration curve using bulk standard Al-Cu alloys. After the verification, using the MC simulation, we suggest the quantitative analysis method for measuring the trace elements in the thin Al films. Also, the MC simulation we developed does not consider a fluorescence correction. We will discuss later the effect of the fluorescence correction for trace elements in an aluminum matrix.

## 2. Monte Carlo simulation

A MC simulation pursues electron trajectories, which enable us to calculate both the production of characteristic X-rays along the electron trajectories and the absorption correction of the generated characteristic X-rays. In order to calculate the electron trajectories, we used the screened Rutherford cross section for elastic scattering [1], the Bethe equation [2], the Rao-Sahib and Wittry equation [3] for energy loss, the ionization cross section by Green and Cosslett [4] and the fluorescence yield by Laberrigue-Frolow and Radvanyi [5]. The calculation of electron trajectories was stopped

0022–2461

TABLE I Chemical analysis results of samples (mass ppm)

| Sample | Cu | Si | Fe | Ti | Mn | Mg | Al |
|---|---|---|---|---|---|---|---|
| No. 1 | 99 | <1 | <1 | <1 | <1 | <1 | Bal. |
| No. 2 | 310 | <1 | <1 | <1 | <1 | <1 | Bal. |
| No. 3 | 1000 | <2 | <2 | <1 | <1 | <1 | Bal. |

either when the electron escaped from the targets into the vacuum or when the electron energy was below the critical excitation energy. This MC code has been already described in detail [6, 7].

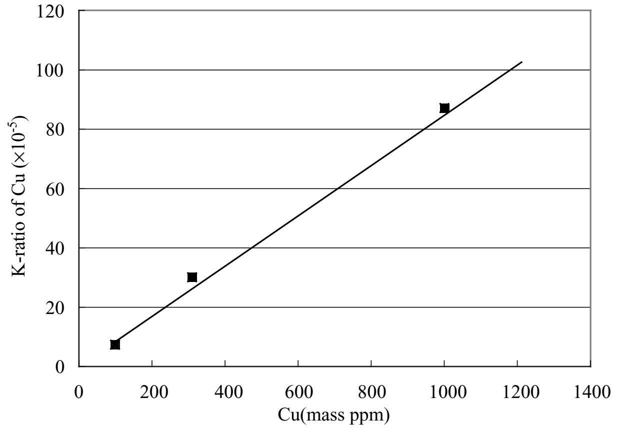

*Figure 1* Calibration curve (■: experimental value).

## 3. Results

### 3.1. Verification of MC simulation

To verify the calibration curve made with the MC simulation, we prepared three kinds of bulk standard Al-Cu alloys. The chemical compositions of each sample are shown in Table I. From Table I, the concentrations of Cu for No. 1, No. 2 and No. 3 samples were 99,310, and 1000 mass ppm, respectively. Before doing experiments, we checked the variation of the Cu concentration of each sample with EPMA line analysis. As a result, each sample was almost uniform in concentration over the area of 500 × 500 $\mu$m investigated. On the other hand, to determine a calibration curve [K-ratio(Cu) vs mass ppm(Cu) in bulk Al targets], we calculated the K-ratio(Cu) for three Cu concentration of 100, 600, 1200 mass ppm in the bulk Al targets. Here, the K-ratio is the ratio between the X-ray production of an element in a bulk target following absorption and the X-ray production of the same element in a bulk standard target following absorption. The calculated conditions are the initial energy of the electron 15 keV, the numbers of trajectories 1500, the beam incidence angle 0° (normal incidence) and the take-off X-ray 52.5° from the sample surface. Table II shows the physical parameters of Cu, Al required for the MC calculation. We used the excitation potential values written by Kemp [8] and the mass attenuation coefficient values written by Veigele [9]. The results are shown in Table III. The relation between the averaged K-ratio of Cu and the Cu concentration (mass ppm) is shown in Fig. 1. In the Fig. 1, the horizontal axis and the vertical axis show the Cu concentration (mass ppm) and the K-ratio of Cu, respectively. Next, we measured the X-ray profile of Cu for the standard, No. 1 and No. 3 samples. The results are shown in Fig. 2a, b and c. As a result, the peak wavelength was 1.544 Å, the upper background wavelength 1.560 Å and the lower background wavelength 1.524 Å. After that, using those wavelengths, we measured the X-ray intensities of each sample. The experimental conditions were the electron–beam current 20 nA, an accelerating voltage 15 kV, the beam incidence angle 0° (normal incidence), the measuring time 200 s for samples and 20 s (to prevent off–scale) for pure Cu. Next, the averaged background X-ray intensity was obtained by averaging the upper and the lower background X-ray intensities. The real X-ray intensities of Cu were obtained by subtracting the averaged background X-ray intensities from the peak X-ray intensities. The experimental results are shown in Table IV. After that the relative X-ray intensities were calculated. The relative X-ray intensity is the ratio between the X-ray intensity of an element in the bulk sample and the X-ray intensity of the same element of a bulk standard sample. The results are shown in Table V. Also, the K-ratio is corresponding to the relative X-ray intensity, from this, the averaged relative X-ray intensities in Table V were plotted on the calibration curve in Fig. 1. Consequently, we found the MC simulation is in good agreement with the experiment.

### 3.2. Quantitative analysis method of trace element in thin film

#### 3.2.1. *Electron trajectories (X-ray production region) in thin film*

The state of the X-ray production generated from thin films becomes different from that of bulk samples, because mainly the excitation potential of elements involved in thin films is different. The excitation potential is the minimum potential to generate characteristic X-ray line. Here, the X-ray production region in Al-Cu (1000 mass ppm) for bulk, 0.8 $\mu$m, 0.6 $\mu$m, 0.4 $\mu$m

TABLE II Physical parameters used for Al, Cu

| Element | Excitation potential (keV) | Atomic number | Atomic weight | Mass attenuation coefficient ($\mu/\rho$) | | Density (g/cm$^3$) |
|---|---|---|---|---|---|---|
| Al (K$\alpha$) | 1.559 | 13 | 26.98 | Al→Al | 407 | 2.7 |
| | | | | Al→Cu | 4520 | |
| Cu (K$\alpha$) | 8.98 | 29 | 63.546 | Cu→Cu | 55 | 8.93 |
| | | | | Cu→Al | 50 | |
| | | Al-Cu alloys | | | | 2.7 |

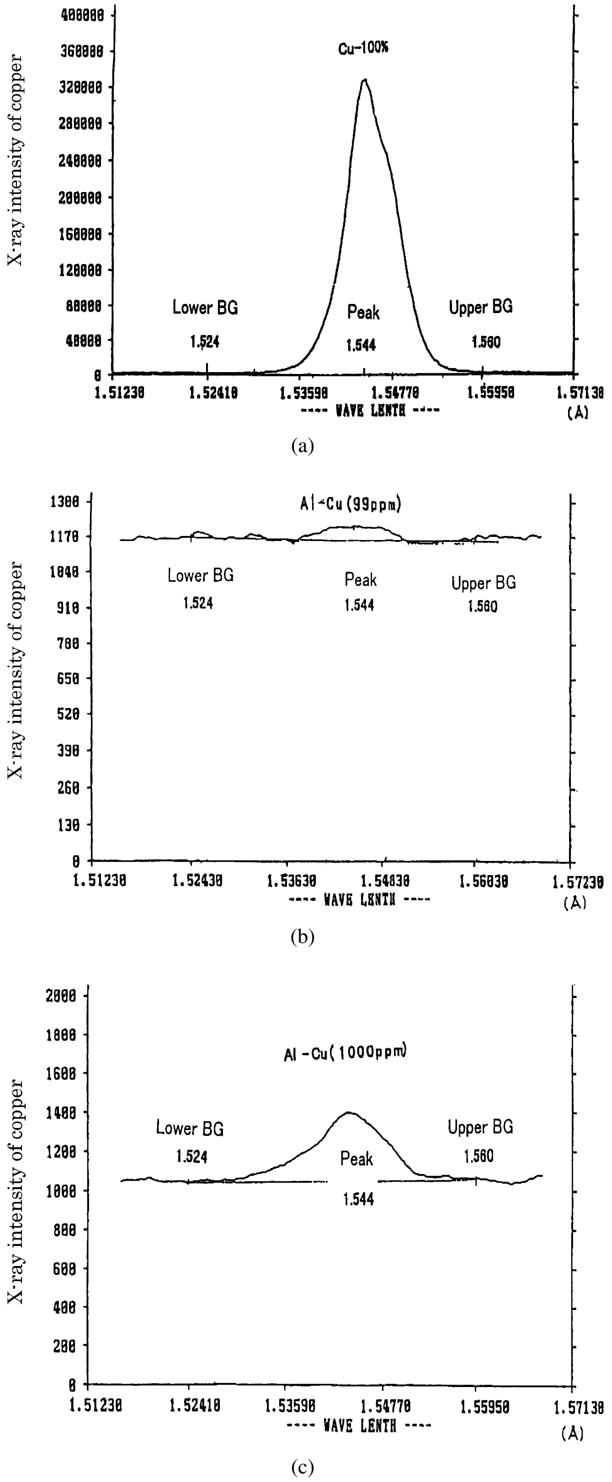

(a)

(b)

(c)

*Figure 2* (a) Pure Cu(K$\alpha$) X-ray profile. (15 kV, 20 nA, 20 s). (b) Cu(K$\alpha$) X-ray profile of Al-Cu (99 mass ppm). (15 kV, 20 nA, 20 s). (c) Cu(K$\alpha$) X-ray profile of Al-Cu (1000 mass ppm). (15 kV, 20 nA, 20 s).

and 0.2 $\mu$m in thickness are shown in Fig. 3. In the figures (a), (b), (c), (d), we can admit the red and the blue contrast trajectories. The red contrast shows the X-ray production region from Al and Cu, and the blue contrast shows the X-ray production region from Al. However, in the figure (e), we can not admit the blue contrast trajectories. From Fig. 3, we can admit that the X-ray productions generated from thin films decrease with the decreasing of the film thickness and the state of the X-ray production becomes different from the film thickness.

TABLE III Calculated results of Cu K-ratio

| Al-Cu (100 mass ppm) | Al-Cu (600 mass ppm) | Al-Cu (1200 mass ppm) |
|---|---|---|
| $8.488 \times 10^{-5}$ | $50.64 \times 10^{-5}$ | $101.64 \times 10^{-5}$ |

TABLE IV Experimental results

| Sample | | X-ray intensities | | | | |
|---|---|---|---|---|---|---|
| | | Time (sec) | Peak (counts) | Lower BG (counts) | Upper BG (counts) | Real (counts) |
| Pure Cu | 1 | 20 | 342804 | 3820 | 3323 | 389532 |
| | 2 | 20 | 344020 | 3807 | 3201 | 340516 |
| | 3 | 20 | 342156 | 3944 | 3322 | 338523 |
| | 4 | 20 | 343406 | 3765 | 3299 | 339874 |
| | 5 | 20 | 344431 | 3911 | 3411 | 340770 |
| | av. | - | 343363 | 3849 | 3311 | 339783 |
| No. 1 | 1 | 200 | 11808 | 11641 | 11492 | 241 |
| | 2 | 200 | 11880 | 11649 | 11571 | 330 |
| | 3 | 200 | 11914 | 11699 | 11643 | 243 |
| | 4 | 200 | 11877 | 11692 | 11573 | 239 |
| | 5 | 200 | 11897 | 11712 | 11598 | 242 |
| | av. | - | 11875 | 11679 | 11575 | 247 |
| No. 2 | 1 | 200 | 12605 | 11694 | 11494 | 1011 |
| | 2 | 200 | 12619 | 11602 | 11481 | 1077 |
| | 3 | 200 | 12635 | 11598 | 11490 | 1091 |
| | 4 | 200 | 12557 | 11572 | 11395 | 1073 |
| | 5 | 200 | 12573 | 11621 | 11382 | 1071 |
| | av. | - | 12598 | 11617 | 11448 | 1065 |
| No. 3 | 1 | 200 | 14524 | 11509 | 11491 | 3024 |
| | 2 | 200 | 14465 | 11602 | 11566 | 2881 |
| | 3 | 200 | 14452 | 11587 | 11411 | 2953 |
| | 4 | 200 | 14593 | 11697 | 11513 | 2988 |
| | 5 | 200 | 14512 | 11707 | 11401 | 2958 |
| | av. | - | 14509 | 11620 | 11476 | 2961 |

TABLE V Experimental results of averaged relative X-ray intensity

| No. 1 | No. 2 | No. 3 |
|---|---|---|
| $7.3 \times 10^{-5}$ | $31.3 \times 10^{-5}$ | $87.1 \times 10^{-5}$ |

### 3.2.2. Quantitative analysis method

The X-ray generation ratio was defined as the ratio between the X-ray production of an element in a film target and the X-ray production of the same element in the same bulk target. We studied the trace elements such as Mg, Si, Ti, Cr, Mn, Fe, Ni, Cu, Zn in the thin Al films. The 100, 600, 1200 mass ppm in concentration and 0.8, 0.6, 0.4, 0.2 $\mu$m in thickness were used. We investigated the relation among the X-ray generation ratio, the trace element concentration and the film thickness. The calculated conditions are the initial energy of the electron 15 keV, the numbers of trajectories 1500, the beam incidence angle 0° (normal incidence) and the take-off angle of X-ray 52.5° from the sample surface. Tables VIa–h show the physical parameters for the MC calculation. The results of the X-ray generation ratio are shown in Figs 4a–12a. From the figures, we found that the X-ray generation ratio was in relation to the film thickness, however it was not in relation to the concentration of trace element. Namely, from

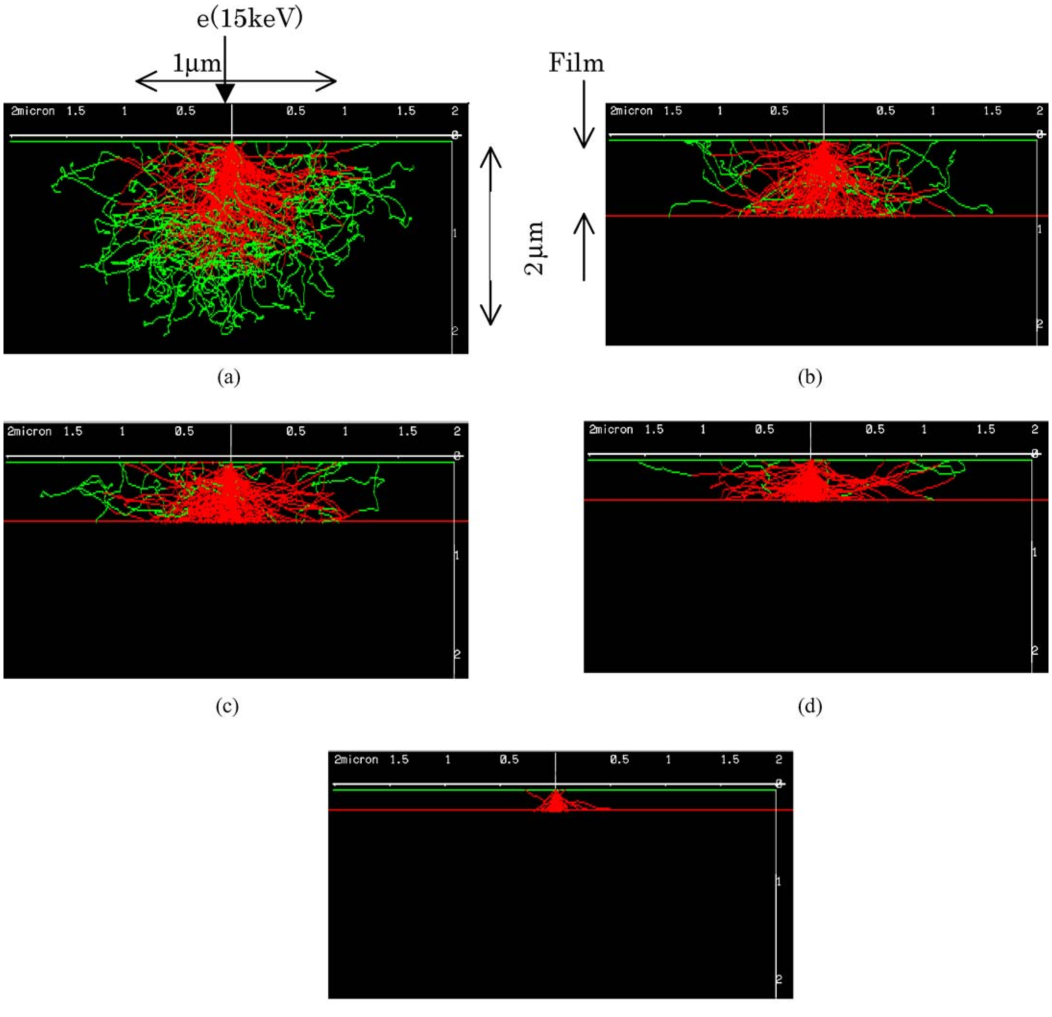

(a) (b) (c) (d) (e)

*Figure 3* Electron trajectories (X-ray production region) of Al-Cu alloys. (a) Al-Cu (1000 mass ppm)(bulk). The red contrast shows the X-ray production region from Al and Cu, and the blue contrast shows the X-ray production region from Al. (b) Electron trajectories of 0.8 $\mu$m thickness [Al-Cu (1000 mass ppm)]. (c) Electron trajectories of 0.6 $\mu$m thickness [Al-Cu (1000 mass ppm)]. (d) Electron trajectories of 0.4 $\mu$m thickness [Al-Cu (1000 mass ppm)]. (e) Electron trajectories of 0.2 $\mu$m thickness [Al-Cu (1000 mass ppm)].

our experiment, if the thickness of unknown samples is known, using the X-ray generation ratio we can transfer from relative X-ray intensity of the film into the relative X-ray intensity of the bulk sample. Finally, using calibration curves (K-ratio vs mass ppm) we can obtain the concentration (mass ppm) of trace elements in the films, because K-ratio is corresponding to the relative X-ray intensity. Figs 4b–12b show calibration curves (K-ratio vs mass ppm) for Mg, Si, Ti, Cr, Mn, Fe, Ni, Cu, Zn in the bulk Al matrix.

### 3.2.3. *Detectable minimum film thickness*

The detectable minimum film thickness is mainly decided with the performances of EPMA, the kinds of element, experimental conditions and so on. Here we try to discuss the Cu in Al-Cu alloys. From Table IV, we can see that the 99, 310, 1000 mass ppm are corresponding to 247, 1065, 2961 counts, respectively. Here, the 247 counts were assumed to be the detectable minimum X-ray intensity. We tried to calculate the X-ray intensity from the 0.4 $\mu$m thickness [Al-Cu (310 mass ppm)]. From Fig. 11a, the X-ray generation ratio of 0.4 $\mu$m thickness is 0.48. Consequently, the X-ray intensity of the 0.4 $\mu$m thickness [Al-Cu (310 mass ppm)] is obtained as 511 (1065 × 0.48) counts. From this, it was found that we detect the Cu concentration in 0.4 $\mu$m thickness [Al-Cu (310 mass ppm)]. Similarly, the X-ray generation ratio of 0.2 $\mu$m thickness is 0.22. Consequently, the X-ray intensity of the 0.2 $\mu$m thickness [Al-Cu (1000 mass ppm)] is obtained as 651 (2961 × 0.22) counts. From this, it was found that we detect the Cu concentration in 0.2 $\mu$m thickness [Al-Cu (1000 mass ppm)].

## 4. Fluorescence correction for trace elements in aluminum matrix

To carry out the fluorescence correction for trace elements in the aluminum matrix, we assumed Al-1%Mg, 1%Si, 1%Ti, 1%Cr, 1%Mn, 1%Fe, 1%Ni, 1%Cu, 1%Zn alloy and calculated it by the Reed's method [10]. The results are shown in Table VII. As a result, the correction effects of the fluorescence for Al, Si, Cu and Zn were found to be negligible and for the other trace elements it were below about 5%.

TABLE VI

| Element | Excitation potential (keV) | Atomic number | Atomic weight | Mass attenuation coefficient ($\mu/\rho$) | Density (g/cm$^3$) |
|---|---|---|---|---|---|
| (a) Physical parameters used for Al, Mg | | | | | |
| Al (K$\alpha$) | 1.559 | 13 | 26.98 | Al→Al 407 | 2.7 |
| | | | | Al→Mg 4390 | |
| Mg (K$\alpha$) | 1.30 | 12 | 24.305 | Mg→Mg 506 | 1.74 |
| | | | | Mg→Al 663 | |
| | | Al-Mg alloys | | | 2.7 |
| (b) Physical parameters used for Al, Si | | | | | |
| Al (K$\alpha$) | 1.559 | 13 | 26.98 | Al→Al 407 | 2.7 |
| | | | | Al→Si 552 | |
| Si (K$\alpha$) | 1.838 | 14 | 28.08 | Si→Si 360 | 2.34 |
| | | | | Si→Al 3440 | |
| | | Al-Si alloys | | | 2.7 |
| (c) Physical parameters used for Al, Ti | | | | | |
| Al (K$\alpha$) | 1.559 | 13 | 26.98 | Al→Al 407 | 2.7 |
| | | | | Al→Ti 2130 | |
| Ti (K$\alpha$) | 4.95 | 22 | 47.90 | Ti→Ti 120 | 4.60 |
| | | | | Ti→Al 279 | |
| | | Al-Ti alloys | | | 2.7 |
| (d) Physical parameters used for Al, Cr | | | | | |
| Al (K$\alpha$) | 1.559 | 13 | 26.98 | Al→Al 407 | 2.7 |
| | | | | Al→Cr 2740 | |
| Cr (K$\alpha$) | 5.98 | 24 | 51.996 | Cr→Cr 94 | 7.20 |
| | | | | Cr→Al 163 | |
| | | Al-Cr alloys | | | 2.7 |
| (e) Physical parameters used for Al, Mn | | | | | |
| Al (K$\alpha$) | 1.559 | 13 | 26.98 | Al→Al 407 | 2.7 |
| | | | | Al→Mn 3420 | |
| Mn (K$\alpha$) | 6.54 | 25 | 54.938 | Mn→Mn 76 | 7.42 |
| | | | | Mn→Al 99 | |
| | | Al-Mn alloys | | | 2.7 |
| (f) Physical parameters used for Al, Fe | | | | | |
| Al (K$\alpha$) | 1.559 | 13 | 26.98 | Al→Al 407 | 2.7 |
| | | | | Al→Fe 3420 | |
| Fe (K$\alpha$) | 7.11 | 26 | 55.847 | Fe→Fe 76 | 7.85 |
| | | | | Fe→Al 99 | |
| | | Al-Fe alloys | | | 2.7 |
| (g) Physical parameters used for Al, Ni | | | | | |
| Al (K$\alpha$) | 1.559 | 13 | 26.98 | Al→Al 407 | 2.7 |
| | | | | Al→Ni 4260 | |
| Ni (K$\alpha$) | 8.29 | 28 | 58.71 | Ni→Ni 63 | 8.85 |
| | | | | Ni→Al 63 | |
| | | Al-Ni alloys | | | 2.7 |
| (h) Physical parameters used for Al, Zn | | | | | |
| Al (K$\alpha$) | 1.559 | 13 | 26.98 | Al→Al 407 | 2.7 |
| | | | | Al→Zn 4960 | |
| Zn (K$\alpha$) | 9.65 | 30 | 65.37 | Zn→Zn 51 | 7.12 |
| | | | | Zn→Al 41 | |
| | | Al-Zn alloys | | | 2.7 |

TABLE VII Calculated results of fluorescence correction value for trace elements such as 1%Mg, 1%Si, 1%Ti, 1%Cr, 1%Mn, 1%Fe, 1%Ni, 1%Cu, 1%Zn in bulk Al matrix (at 15 kV)

| Element | Fluorescence correction value | Element | Fluorescence correction value |
|---|---|---|---|
| Mg | 0.951 | Fe | 0.996 |
| Si | 1.000 | Ni | 0.995 |
| Ti | 0.996 | Cu | 1.000 |
| Cr | 0.996 | Zn | 1.000 |
| Mn | 0.997 | Al | 1.000 |

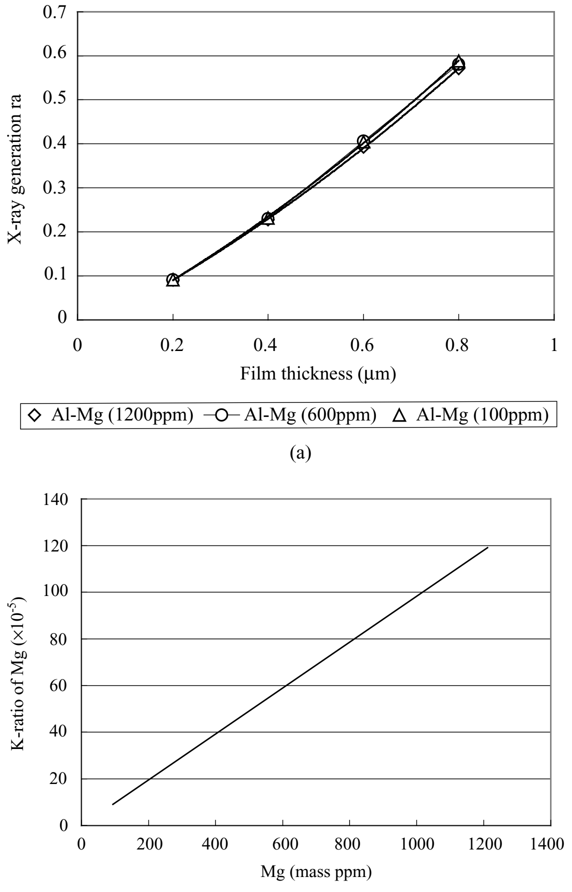

(a)

(b)

*Figure 4* (a) X-ray generation ratio of Mg. (b) Calibration curve of Mg.

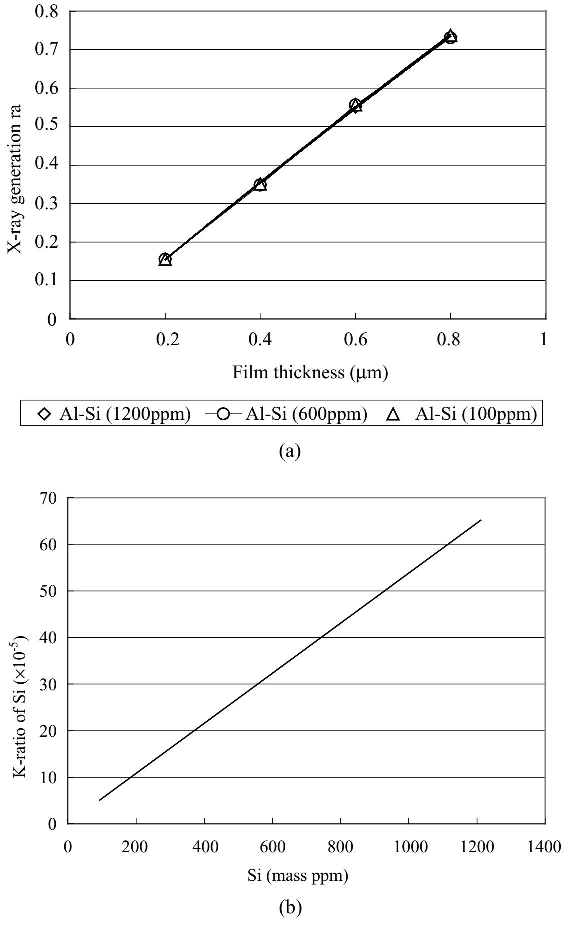

(a)

(b)

*Figure 5* (a) X-ray generation ratio of Si. (b) Calibration curve of Si.

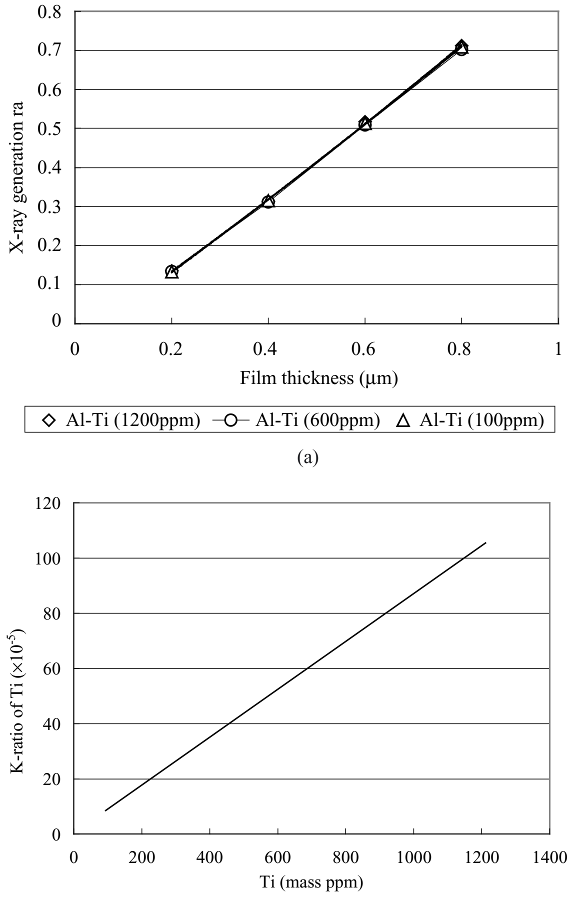

(a)

(b)

*Figure 6* (a) X-ray generation ratio of Ti. (b) Calibration curve of Ti.

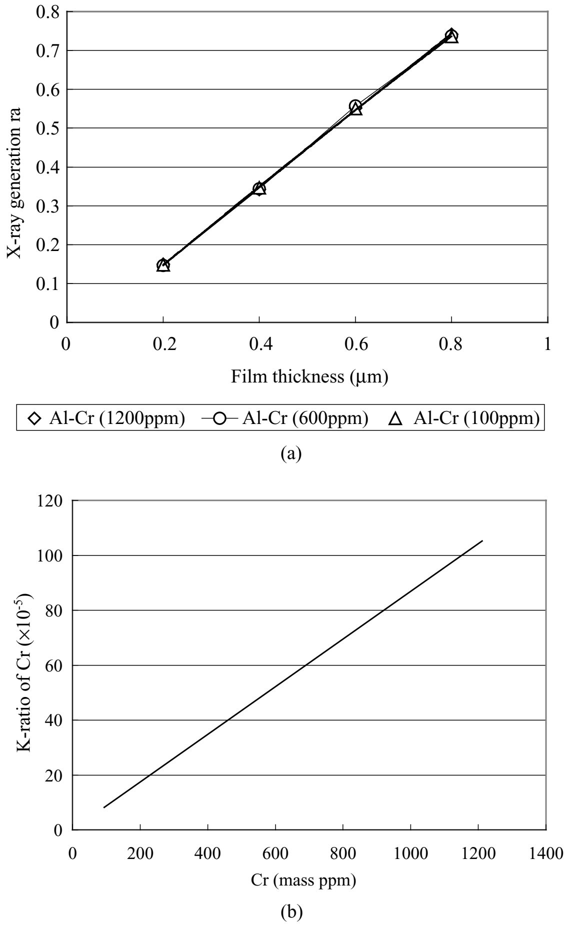

(a)

(b)

*Figure 7* (a) X-ray generation ratio of Cr. (b) Calibration curve of Cr.

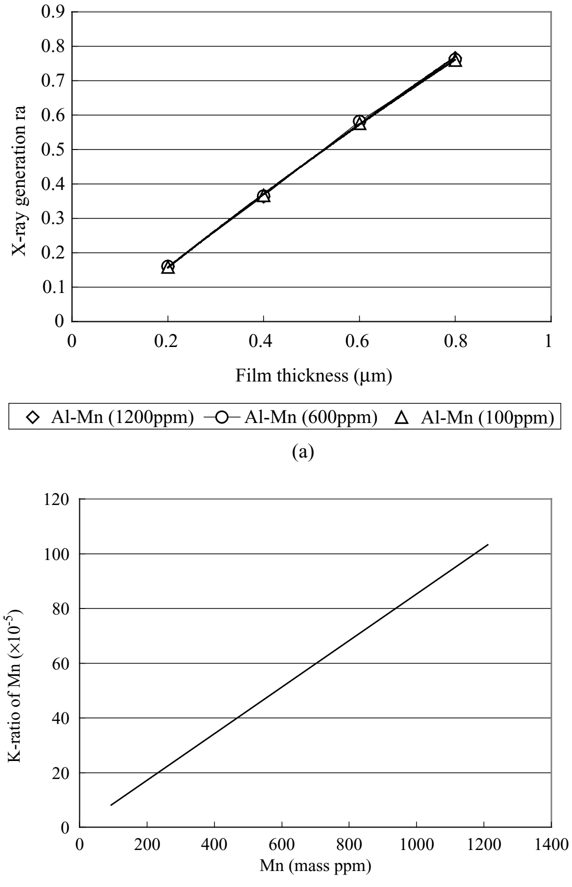

(a)

(b)

*Figure 8* (a) X-ray generation ratio of Mn. (b) Calibration curve of Mn.

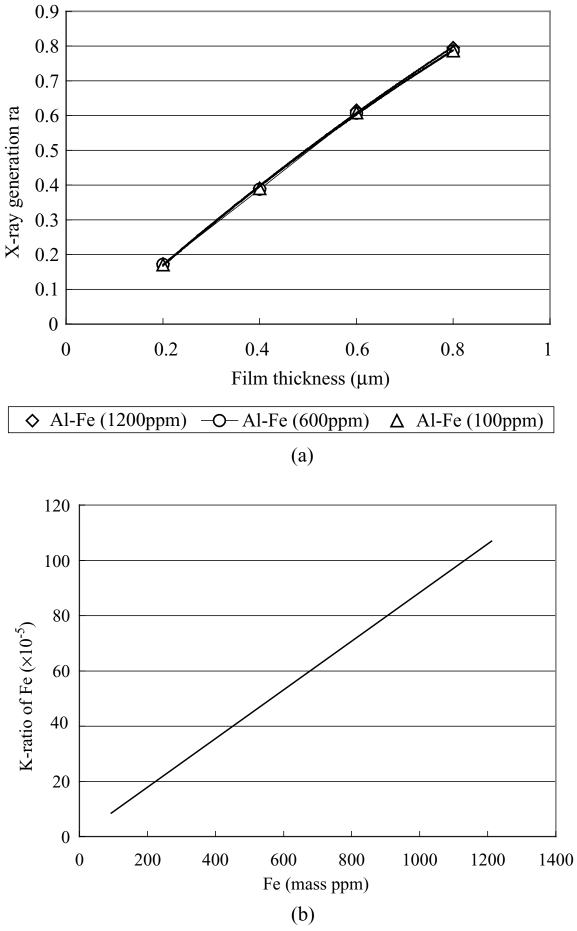

(a)

(b)

*Figure 9* (a) X-ray generation ratio of Fe. (b) Calibration curve of Fe.

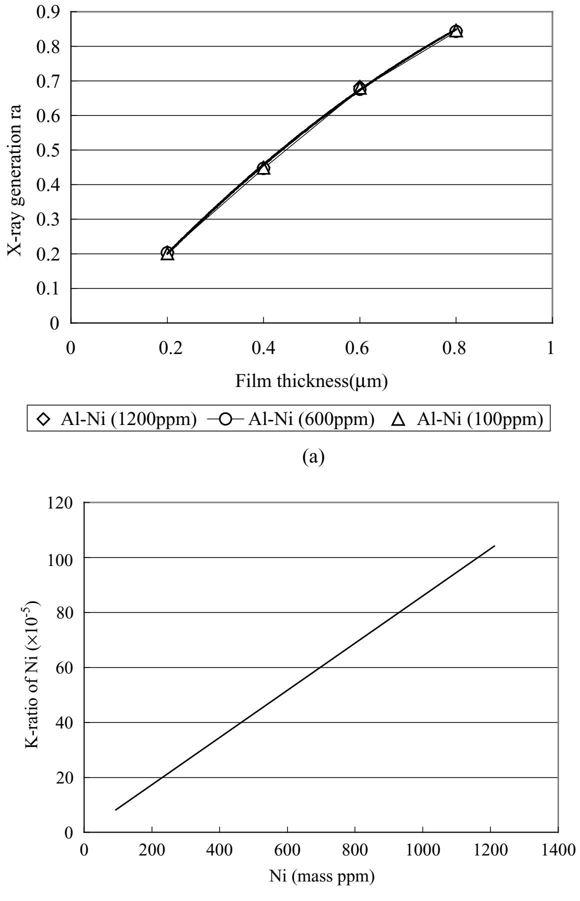

(a)

(b)

*Figure 10* (a) X-ray generation ratio of Ni. (b) Calibration curve of Ni.

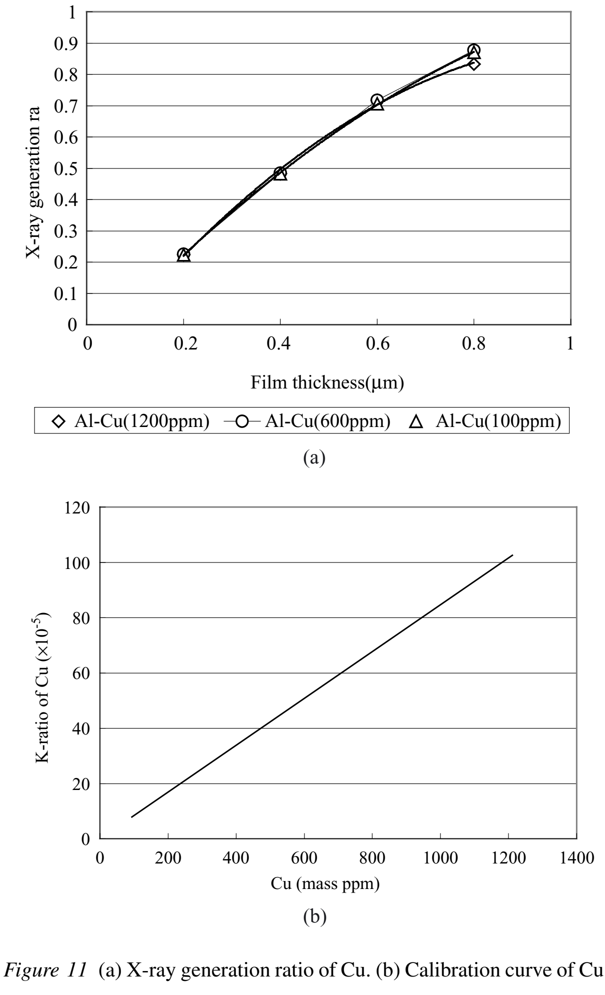

(a)

(b)

*Figure 11* (a) X-ray generation ratio of Cu. (b) Calibration curve of Cu.

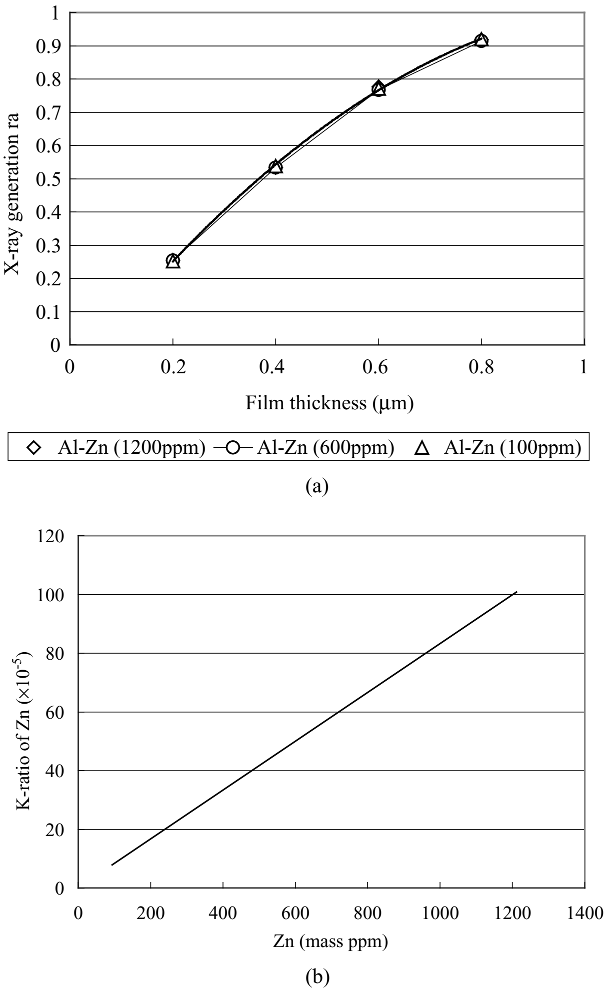

(a)

(b)

*Figure 12* (a) X-ray generation ratio of Zn. (b) Calibration curve of Zn.

## 5. Conclusion

In this paper, MC simulation was applied to the obtaining of the calibration curves and the calculation of the X-ray generation ratio. After verifying the MC simulation, we suggested the quantitative analysis method of trace elements (100–1200 mass ppm) in thin Al films and provided the X-ray generation ratios and the calibration curves (K-ratio vs mass ratio) of trace elements such as Mg, Si, Ti, Cr, Mn, Fe, Ni, Cu, Zn in the bulk Al matrix.

## Acknowledgments

The author wishes to thank Professor Kenji Murata of Osaka Prefecture University for his valuable suggestions on Monte Carlo simulation and for his encouragement. Also, the author thanks that samples were provided by Research and Development Center of Nippon Light Metal Co. Ltd.

## References

1. K. MURATA, T. MATSUKAWA and R. SHIMIZU, in Proceeding of the Sixth International Conference on X-ray Optics microanalysis (Tokyo, 1972) p. 105.
2. H. A. BETHE, *Ann. Physik (Leipzig)* **5** (1930) 325.
3. T. RAO-SAHIB and D. B. WITTRY, *J. Appl. Phys.* **45** (1974) 5060.
4. M. GREEN and V. E. COSSLETT, *Proc. Phys. Soc.* **78** (1961) 1206.

5. J. LABERRIGUE-FROLOW and P. RADVANYI, *J. Phys. Radium.* **17** (1956) 944.
6. Y. OSADA, *J. Mater. Sci.* **38** (2003) 1457.
7. Y. OSADA, X-ray Spectrometry (2003, in press).
8. J. W. KEMP, “X-ray Wavelength Tables” (Applied Reseach Laboratories, Inc).
9. WILLIAM J. VEIGELE, in cm2/g At Selected Wavelength for 94 Elements (Kamam Science Corporation).
10. S. J. B. REED, *Brit. J. Appl. Phys.* **16** (1965) 913.

*Received 19 January*
*and accepted 20 September 2004*